Sliding Mode Control of the MMC-based Power System

Aghahadi, Morteza; Piegari, Luigi; Lekic, Aleksandra; Shetgaonkar, Ajay

DOI
10.1109/IECON49645.2022.9968871

Publication date
2022

Document Version
Final published version

Published in
IECON 2022 - 48th Annual Conference of the IEEE Industrial Electronics Society

Sliding Mode Control of the MMC-based Power System

IECON 2022 – 48th Annual Conference of the IEEE Industrial Electronics Society | 978-1-6654-8025-3/22/$31.00 ©2022 IEEE | DOI: 10.1109/IECON49645.2022.9968871

Morteza Aghahadi, Luigi Piegari,
Department of Electronics, Information and Bioengineering, Politecnico di Milano,
Milan, Italy
morteza.aghahadi@mail.polimi.it, luigi.piegari@polimi.it

Aleksandra Lekić, Ajay Shetgaonkar,
Intelligent Electrical Power Grids, Faculty of Electrical Engineering, Mathematics and Computer Science, TU Delft
Delft, Netherlands,
A.Lekic@tudelft.nl, A.D.Shetgaonkar@tudelft.nl

***Abstract*— The modular multilevel converter has become a popular topology for many applications in medium and high-power conversion systems such as multi-terminal direct current power systems. In this paper, Modular multilevel converter structure and related equations are presented. Then, control methods for circulating current, output current, and energy balance among legs and upper and lower arms of each phase for conventional proportional-integral control and sliding mode control are described. Notably, this study concentrates on the multi-terminal direct current configuration link with master-slave control by presenting a π model for the high voltage direct current transmission line. Moreover, dq-frame is used in the control strategy with a modified first-order sliding mode control and a second-order sliding mode control for preventing chattering. The results show that applying the proposed method in a hybrid power system can provide fast transient responses, zero overshoot, and better stability. Finally, the results are verified by simulations in MATLAB/Simulink.**

Keywords*— Modular multilevel converter, Multi-terminal DC power systems, Master-slave, Sliding mode control.

I. INTRODUCTION

There are many technologies in high voltage direct current (HVDC) applications but using voltage source converter (VSC) technology has become the most developed converter topology in recent years [1]. In VSC, active-reactive power control is performed by controlling the current instead of DC voltages, hence it enables multi-terminal configuration. Further, VSC has a bidirectional capability, and the active and reactive power can be controlled independently [2]. VSCs with a higher than two levels have better performances in terms of voltage stress and harmonic distortion [3]. Modular multilevel converters (MMCs) have many submodules that have lower-level switching losses in comparison with 2-level and 3-level VSCs [4].

Lately, the multi-terminal direct current (MTDC) configuration has become a popular configuration to transmit large electrical power in DC systems between countries with underground cables because of some advantages such as controllability, easier improvement, low losses, and having a common voltage controlled by master MMC [5]. However, the control of MMC is complicated because of its topology associated with extra degrees of freedom in comparison with 2-level and 3-level VSCs.

There are different control strategies to manage the current and power of MMCs. The proportional-integral (PI) and proportional resonant controllers have been applied for the control of MMCs. However, the performance of both controllers can be degraded when power fluctuates considerably. [6]- [7]. Non-linear controllers such as predictive controls have been applied to regulate the grid current of MMCs. It might be overworked in terms of computation. Although optimality can be reached, stability cannot be guaranteed [8].

Sliding mode control (SMC) is one of the sub-branches of robust controls and has recently become popular recently because of some remarkable characteristics such as easy implementation, easy tunning, and better stability.

In this paper, an energy-based controlled approach [9] [1] is considered based on traditional PI control and SMC for a hybrid power system. The controller model for output current (OC) (active-reactive power control) is based on the first-order SMC [10], [11], and two kinds of second-order SMC(SOSMC) called super-twisting SMC (STSMC), and prescribed law of convergence of sliding (PLCS) algorithm [11] [12]. Additionally, STSMC is applied to regulate capacitor voltage, and balance the energy in the arms which improves the performance especially in worse scenarios. The proposed controllers, compared with linear approaches show a fast dynamic response and better steady state performance. Finally, the control structure is validated in MATLAB/Simulink.

II. SYSTEM DESCRIPTION:

The analyzed system (Fig.1) is considered with four MMCs connected to a the MTDC scheme and four AC grids.

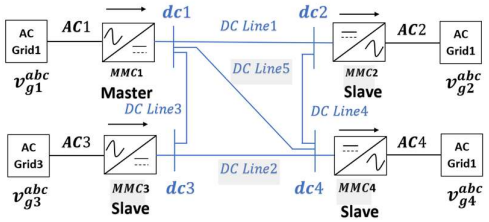

Fig. 1. The MTDC system under study

In the master-slave control approach, the master MMC regulates the voltage across the system, slave MMCs are responsible for controlling active power flows. Reactive power can also be controlled by all MMCs independently [13].

In a typical MMC (Fig.2), there are three legs and three phases equivalently. Each leg has two arms with N_{arm} half-bridge submodules connected to a capacitor (C_{sm}). The key point of the control scheme is to calculate the voltages of six arms (v_{ul}^{abc}) for balancing the energy to avoid extra energy losses in the MMC and to exchange the power from the AC side to the DC side or vice versa in a smooth way.

Note: This notation (v_{ul}^{abc}) is used for expressing the variables in this paper for example: $x_{ul}^{abc} = (x_u^a, x_u^b, x_u^c, x_l^a, x_l^b, x_l^c,)^T$.

A typical control scheme for the MMC is shown in Fig. 3. At the top, the output current control is presented consisting of a voltage controller for master MMC, or an active power controller for slave MMC and reactive power control for both.

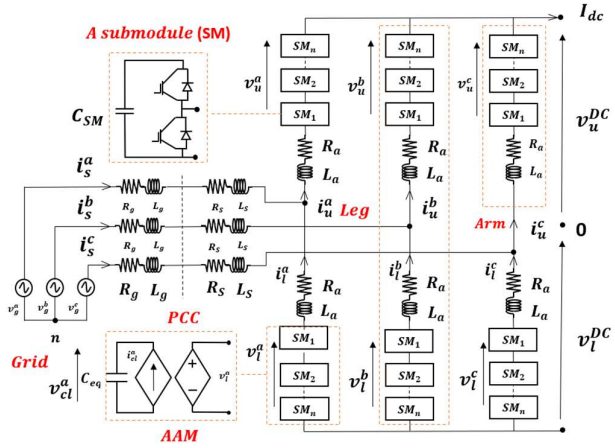

Fig. 2. Circuit diagram of the MMC and the grid Thevenin equivalent.

At the bottom, the circulating current (CC) and energy balancing control are presented. At the top-left, a phase-locked loop (PLL) is presented that can estimate an angle between grid voltage and point of common connection (PCC) for control loops.

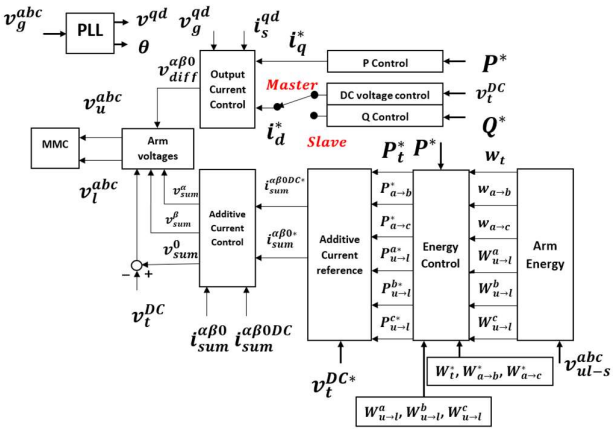

Fig. 3. A typical control scheme of MMC

III. DYNAMIC MODELING OF THE SYSTEM:

A. MMC and Grid

Applying the KVL to each phase $(k = a, b, c)$, it is possible to write:

$$v_u^{DC} - v_u^k - v_g^k - v_n = R_a i_u^k + L_a \frac{di_u^k}{dt} + \left(R_s + R_g\right) i_s^k + \left(L_s + L_g\right) \frac{di_s^k}{dt} \quad (1)$$

$$-v_l^{DC} - v_l^k - v_g^k - v_n = -R_a i_l^k - L_a \frac{di_l^k}{dt} + \left(R_s + R_g\right) i_s^k + \left(L_s + L_g\right) \frac{di_s^k}{dt} \quad (2)$$

Where the lower and upper arms, and grid currents for the generic k phase are indicated by i_l^k, i_u^k, and i_s^k respectively. The resistances and inductances of the grid and arm are denoted by R_g, R_a, L_g, and L_a. Furthermore, the voltages related to the DC side, grid, and arm are denoted by v_u^{DC}, v_l^{DC}, v_g^k, and v_u^k, v_l^k respectively.

To obtain the expressions that describe the differential and additive quantities, it is necessary to sum and subtract equations (1) and (2). These equations provide useful insights into the way MMC works. Additionally, these diagonalize the dynamic operation and can decouple voltage and current variables. New variables are defined as follows:

$v_{diff}^k \triangleq 0.5\,(-v_u^k + v_l^k)$, differential voltage. $v_{sum}^k \triangleq v_u^k + v_l^k$, additive voltage. $i_{sum}^k \triangleq 0.5\,(i_u^k + i_l^k)$, additive current

$R_{eq} \triangleq R_s + R_g + \frac{R_a}{2}$. $L_{eq} \triangleq L_s + L_g + \frac{L_a}{2}$. ($R_s$, L_s are neglected as just slight voltage drop)

$v_t^{DC} \triangleq v_u^{DC} + v_l^{DC}$, $(v_u^{DC} \approx v_l^{DC})$.

Therefore, MMC can be defined by two equations as follows:

$$v_{diff}^k - v_g^k - v_{n0} = R_{eq} i_s^k + L_{eq} \frac{di_s^k}{dt} \quad (3)$$

Differential equation interprets the relation of the MMC and AC side.

$$v_{sum}^k - v_t^{DC} = -2R_{eq} i_{sum}^k - 2L_{eq} \frac{di_{sum}^k}{dt} \quad (4)$$

The additive equation interprets the relation of the MMC and circulating currents. Equations (3), (4) can identify the key degrees of freedom of MMC and helps to design the controller more conveniently. Generally, the currents i_{sum}^k and i_s^k have AC and DC components. Indeed, each of the components has a special responsibility [7] in control of MMC and power exchange.

For control purposes, it is suggested to analyze these currents in positive, negative, and zero sequences.

According to the average arm model (AAM), the relation between charging current and real capacitor voltage for six arms when power is exchanged can be expressed as [1]:

$$i_{Cul}^{abc} = C_{eq} \boldsymbol{I_6} \frac{dV_{Cul}^{abc}}{dt} \quad (5)$$

Where, $\boldsymbol{I_6} \in \mathcal{R}^{6\times6}$, is an identity matrix.

B. Control System

B.1. Overview

In general, the designing control system is done in a synchronous reference dq -frame to control active and reactive power separately. The overall scheme is presented in Fig. 3. If PLL is locked properly ($v_g^d = 0$), the active and reactive power references can be calculated as follows:

$$i_q^* = \frac{2}{3}\frac{P^*}{v_g^q}, i_d^* = \frac{2}{3}\frac{Q^*}{v_g^q} \quad (6)$$

Generally, both equations (6) are used for slave MMCs. But i_q^* must be calculated by a voltage regulator in master MMC to keep reference voltage constant. The equation (3) rewrites in dq-frame by Park transformation as follows:

$$v_{diff}^q = -R_{eq} i_s^q - L_{eq} \frac{di_s^q}{dt} + v_g^q - L_{eq}\omega i_s^d$$

$$v_{diff}^d = -R_{eq} i_s^d - L_{eq} \frac{di_s^d}{dt} + v_g^d + L_{eq}\omega i_s^q \quad (7)$$

Where ω is the grid angular frequency.

As mentioned before, an energy controller should balance the six MMC arms. To do that, total energy and leg horizontal

difference energies calculated based on equation (5) as follows:

$$W_t = W_u^a + W_l^a + W_u^b + W_l^b + W_u^c + W_l^c \quad (8)$$

$$W_{a\to b} = (W_u^a + W_l^a) - (W_u^b + W_l^b)$$
$$W_{a\to c} = (W_u^a + W_l^a) - (W_u^c + W_l^c)$$
$$W_{u\to l}^k = W_u^k - W_l^k$$

Then, the equivalent reference powers P_t^*, $P_{a\to b}^*$, and $P_{a\to c}^*$ can be calculated by the values of equations (8) as well as their reference values. Generally, it can be done by a simple PI controller regarding the equation $\frac{dW}{dt} = P$.

$$W_t^* = 6 * 0.5 \frac{C_{SM}}{N_{cm}} (v_t^{DC*})^2 \quad (9)$$

The calculated reference powers in the abc-frame can be used for calculating the DC grids current (i_{sum}^{0DC*}) and DC circulating current ($i_{sum}^{\alpha\beta DC*}$) in the $\alpha\beta 0$ -frame (Clarke transformation). This concept is shown by matrix equation (10) as follows:

$$\begin{bmatrix} i_{sum}^{\alpha DC*} \\ i_{sum}^{\beta DC*} \\ i_{sum}^{0DC*} \end{bmatrix} = \frac{1}{3v_t^{DC*}} \begin{bmatrix} 0 & 1 & 1 \\ 0 & \sqrt{3} & -\sqrt{3} \\ 1 & 0 & 0 \end{bmatrix} \begin{bmatrix} P_t^* \\ P_{a\to b}^* \\ P_{a\to c}^* \end{bmatrix} \quad (10)$$

Where $v_t^{DC*}$is the reference value of the DC side

Finally, the additive voltages are calculated by the equivalent circuit in $\alpha\beta 0$-frame as follows:

$$\begin{bmatrix} v_{sum}^{\alpha} \\ v_{sum}^{\beta} \\ v_{sum}^{0} \end{bmatrix} - v_t^{DC} \begin{bmatrix} 0 \\ 0 \\ 1 \end{bmatrix} = -2R_a \boldsymbol{I_3} \begin{bmatrix} i_{sum}^{\alpha} \\ i_{sum}^{\beta} \\ i_{sum}^{0} \end{bmatrix} - 2L_a \boldsymbol{I_3} \frac{d}{dt} \begin{bmatrix} i_{sum}^{\alpha} \\ i_{sum}^{\beta} \\ i_{sum}^{0} \end{bmatrix} \quad (11)$$

Where, $\boldsymbol{I_3} \in \mathcal{R}^{3\times 3}$ is the identity matrix

Finally, modulation indices can be calculated using reference voltages v_{ul}^{abc}as follows:

$$m_{ul}^{abc} = \frac{v_{ul}^{abc}}{v_{Cul}^{abc}} \quad (12)$$

B.2. Sliding mode control

It is proven that if there is a surface in state space that is equal to zero, states are inclined to move to this surface and if the system dynamic is stable, states will move to the desired point. In other words, by defining a surface so-called sliding surface, it is possible to work with a simple equation and scalar variables instead of working with the set of differential equations and vector variables.

The sliding surface or switching surface in a first-order system can be defined as follows:

S ≜ error of the system

Generally, the sliding surface is defined with tracking error, therefore, S is inclined to zero, and all states reach desired values that are reference values. When the states reach the surface, the controller for keeping the condition must use the sign function (sign(S)). It leads to chattering phenomena. The sign function is a discontinuous function, and the control law will be discontinuous around S = 0. Indeed, chattering is a big problem for the SMC; it leads to high control activity and can enable the high order modes which are eliminated during modelling. Chattering can be decreased significantly by using high-order SMC [12].

The sliding condition is based on this concept if a signal is positive and the derivative of that is negative, that signal will move to zero and it is defined as follow:

$$S\dot{S} \leq -\eta|S| \quad (13)$$

η is a constant and is one of the parameters of design and $\dot{S}$ is the first derivative of the sliding surface.

Let the system define as in [10] for control purposes:

$$\dot{x} = f(x) + b(x)v \quad (14)$$

$x \in \mathcal{R}^n$ is the vector of outputs of interest like arm currents that is system state and v is defined as the scalar control input. $f(x), b(x)$ are non-linear functions of x. The control input in SMC is defined as follows:

$$v = v_{eq} + v_{sw} \quad (15)$$

v_{eq} can be calculated according to Filippov's Construction of the Equivalent Dynamics [10] by solving the equation $\dot{S}$=0. Moreover, there are many options to find the switching input (v_{sw}) concerning equation (13). But one of the best choices is defined as follows:

$$v_{sw} = -k_1\, sign(S) - k_2 \mathrm{S} \quad (16)$$

The variables k_1 *and* k_2 can be tuned to achieve the best response. Additionally, this equation is modified in this paper, while for the standard first-order SMC, $k_2 = 0$. In fact, the equivalent input holds the system trajectory on the sliding surface, whereas switching input keeps the response near the sliding surface.

B.3. Designing output current control using SMC

Equation (7) shows the dynamic of the output current of MMC. The current error in the dq-frame is defined as:

$$e_q = i_s^{q*} - i_s^q, \quad e_d = i_s^{d*} - i_s^d \quad (17)$$

The sliding surfaces are equal to errors and equivalent inputs can be obtained by solving the set of equations ($\dot{S}$=0). They can be calculated as follows:

$$v_{eq}^q = -R_{eq} i_s^{q*} + v_g^q - L_{eq}\omega i_s^{d*} \quad (18)$$
$$v_{eq}^d = -R_{eq} i_s^{d*} + v_g^d + L_{eq}\omega i_s^{q*}$$

In addition, switching law for a first-order SMC can be defined in this case as:

$$v_{sw}^q = -L_{eq}\left(k_{1q}\, sign(S_q) + k_{2q} S_q\right) \quad (19)$$
$$v_{sw}^d = -L_{eq}\left(k_{1d}\, sign(S_d) + k_{2d} S_d\right)$$

In PLCS algorithm, there is a pre-specified guiding function $g(S)$, that leads to sliding variable proceeds the origin. The switching law is defined as:

$$v_{sw}(x) = \begin{cases} -v_{sw}\,, & |\, v_{sw}| \geq v_0 \\ -V\, sign(\dot{S} - g(S)), & |\, v_{sw}| \leq v_0 \end{cases} \quad (20)$$

Where V is a positive constant, and $g(S)$ is a continuous function except for $S = 0$. It is considered all solutions of $\dot{S} = g(S)$ vanish after a finite period of time. One of the choices can be calculated as:

$$g(S) = -\lambda\sqrt{|S|}sign(S) \quad (21)$$

In addition, the switching law for STSMC is given as:

$$v_{sw} = -L_a(\sqrt{k_3}\sqrt{|S_{cc}|}\,sign(S_{cc}) + 1.1\,k_3\int sign(S_{cc})) \quad (22)$$

And finally, control outputs are represented:

$$v_{diff}^{q} = v_{eq}^{q} + v_{sw}^{q} \quad (23)$$

$$v_{diff}^{d} = v_{eq}^{d} + v_{sw}^{d}$$

The second terms switching inputs lead to states moving to sliding surfaces; they have an inverse relationship with rise time. In addition, oscillation can be decreased by reducing the $, k_{1q}, k_{1d}$. The control scheme is shown in Fig. 4.

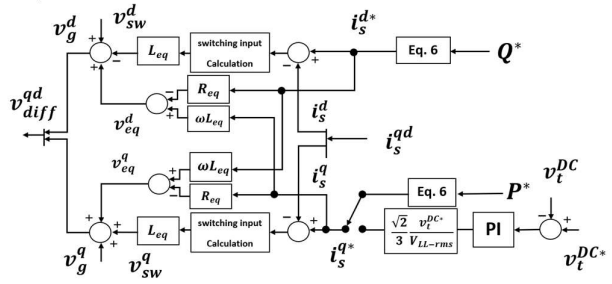

Fig. 4. Control scheme of output current control using SMC

B.4. Circulating current control using SMC

The circulating current does not impact the output currents. Although, it increases the level of losses in MMC. *Circulating current controller only needs the third row of equation (11).* Similarly, the error for circulating current can be defined as:

$$e_{cc} = i_{sum}^{0DC*} - i_{sum}^{0DC} \quad (24)$$

By taking the derivative of the sliding surface that is equal to error and substituting the third equation (11), equivalent input is calculated as:

$$v_{eq}^{cc} = -2\,R_a\,i_{sum}^{0DC*} + v_t^{DC} \quad (25)$$

A second-order SMC is used for circulating current controller called STSMC. The switching law (v_{sw}^{cc}) is defined as [12] the same as equation (22). The control output is defined as:

$$v_{sum}^{0DC} = v_{eq}^{cc} + v_{sw}^{cc} \quad (26)$$

In general, output control has an integral term and continuous nature. So, this controller can reduce the second harmonic current and decrease chattering. The larger value of k_3 can show better performance. Additionally, an increment reference current (Δi_{sum}^{0DC*}) is suggested to add to $i_{sum}^{0D}{}^{*}$ to keep energy arms balanced in [14]. But, in this paper, a simple PI controller is applied for the energy controller. The control scheme is shown in Fig. 5.

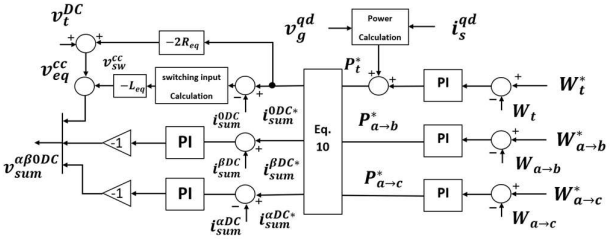

Fig. 5. Control scheme of circulating current control using SMC

C. HVDC line

Underground cable is one of the most important components of HVDC systems. Generally, cable modelling can be divided into two categories. i.e., lumped, and distributed parameter model.

The lumped model can be in the simple and π models which is dependent on the geometry of the transmission line, and it is not suitable for state-space form. The distributed model is created by modelling the cable into N parallel branches and M series circuits. When numbers of n, and m are considered infinite, a wideband, or universal line model (ULM) [15] is proposed which is frequency dependent. Additionally, there are many models that can be found in the best path project [16]. In this paper, an equivalent circuit with $N = 3$, and $M = 1$ is considered for the sake of simplicity (Fig. 6). Moreover, the big capacitor in the DC terminals can improve the DC dynamics.

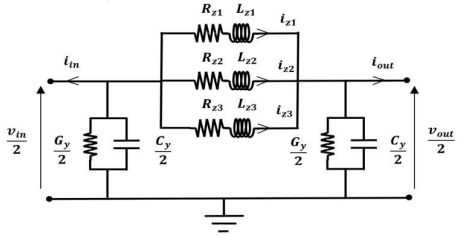

Fig. 6. Equivalent circuit for an underground cable

All the lines in this paper have the same characteristics but with different lengths. The equations related to the model can be written as:

$$\frac{dv_{in}}{dt} = \frac{4}{C_g}\left(-i_{in} - i_{z1} - i_{z2} - i_{z3} - \frac{g_y}{4}V_{in}\right) \quad (27)$$

$$\frac{dv_{out}}{dt} = \frac{4}{C_g}\left(-i_{in} + i_{z1} + i_{z2} + i_{z3} - \frac{g_y}{4}V_{out}\right)$$

$$\frac{di_{zj}}{dt} = \frac{1}{L_{zj}}\left(\frac{V_{in}}{2} - R_{zj}i_{zj} - \frac{V_{out}}{2}\right) \quad (28)$$

Where, V_{in}, V_{out} are the input and output voltages of the cable. i_{ij}, i_{out}, i_{zj} (j = 1,2,3) are input and output currents of the cable flowing through the j branch. C_y, G_y are the equivalent capacitance and admittance respectively. R_{zj}, L_{zj}(j = 1,2,3) are the equivalent resistance and inductance of the j branch. The cable parameters are presented in Table I.

TABLE I. CABLE PARAMETER *[1]*

Symbol	Value	Units	Symbol	Value	Units
r_{z1}	0.1265	$\Omega/_{km}$	l_{z1}	0.2644	$mH/_{km}$
r_{z2}	0.1504	$\Omega/_{km}$	l_{z2}	7.2865	$mH/_{km}$
r_{z3}	0.0178	$\Omega/_{km}$	l_{z3}	3.6198	$mH/_{km}$
c_y	0.1616	$\mu F/_{km}$	g_y	0.1015	$\mu S/_{km}$

IV. RESULTS AND DISCUSSION:

All the data of the simulated system are reported in the Table II.

TABLE II. GRID AND MMC PARAMETERS

Symbol	Value	Units	Symbol	Value	Units
P^*	100	MW	$R_g + j\omega L_g$	0.512 + j18.4412	Ω
Q^*	5	MVAR	$R_a + j\omega L_a$	1.024 + j15.3624	Ω
v_t^{DC}	640	kV	C	9.5	mF
N_{arm}	400	-	ω	314.1593	$rad/_s$

During the case study lasting 3 seconds, two different scenarios are analyzed to depict the performance of the controller. The test is based on loading and disconnecting the load by maximum changes from zero to nominal load or vice versa (the worst cases).

Case A: The active and reactive power demands are connected at t = 0.5 s, and t = 1 s, respectively from 0 % to 100 % nominal load in the system.

Case B: a sudden disconnection of the load from 100% to 0% nominal load at t = 2 s.

MMC1 and MMC3 behave as the power senders, while MMC2 and MMC4 as the power receivers.

For the sake of simplicity, it is assumed that all MMCs and transmission lines have the same characteristics such as modelling and parameters, although they can be different in practical cases. Given this assumption, the power changes in MMC1 and MMC2 are similar. While this behavior is exactly the opposite of MMC2 and MMC4. So, the plots related to power changes can be drawn for only one pair of converters such as receivers' converters.

To have a fair comparison between controllers, output and circulating currents should be tuned such that a fast response based on real modulation limits is obtained [17]. The current controllers are designed for the first-order close loop system response with a time constant equal to 1 ms [6]. For the master converter (MMC1) the PI coefficients are calculated considering the cable equivalent capacitance seen by converter [6] ($k_d = 3 * 10^{-3}, k_i = 77 * 10^{-4}$ respectively). Furthermore, a novel method called optimization robust control is used for slave MMCs with first-order response of 0.1 s [18]. The PLL is tuned with 0.02 s to follow the angle of the grid. Additionally, the coefficients for SMC are listed in Table III.

TABLE III. SMC COEFFICIENTS

Method	Controller	k_{1q}, k_{1d}	k_{2q}, k_{2d}	V	λ	k_3
First-order SMC	OC	0.05	600	-	-	-
PLCS	OC	-	-	20000	3400	-
STSMC	OC	-	-	-	-	4000
	CC	-	-	-	-	80

Fig. 7 compares the ac active and reactive powers using conventional PI and PLCS controllers. Fig. 8 compares the active and reactive using first-order SMC and STSMC. The power difference in the upper-lower arms of each phase and the power difference in legs for PI and STSMC controllers is shown in Fig. 9. Moreover, Fig. 10 shows the voltages in the MTDC system. Finally, Fig. 11 shows the power transfer error convergence for STSMC, showing that SMC can guarantee fast damping with no residual error.

It can be seen in Fig. 7 and Fig. 8 that the STSMC-controlled MMCs have a better response in terms of overshoot and settling time in a transient state as well as steady-state condition. The overshoot with PI is 3.6 times more than STSMC for active power control, while it is more than two times for reactive power control in comparison with STSMC. The settling time related to active power for PI-controlled MMC is 0.25 s, while for STSMC-controlled MMC is 0.05 s. Moreover, settling time can experience a similar trend to reactive power.

The dynamic response presented in Fig 7(b) shows that active power experiences no overshoot with STSMC.

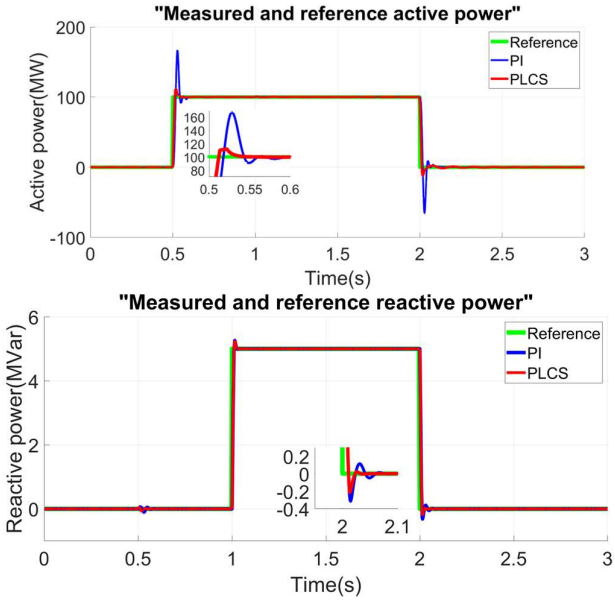

Fig. 7. Power responses for case A and B using PI and PLCS controllers: (a) active power (b) reactive power

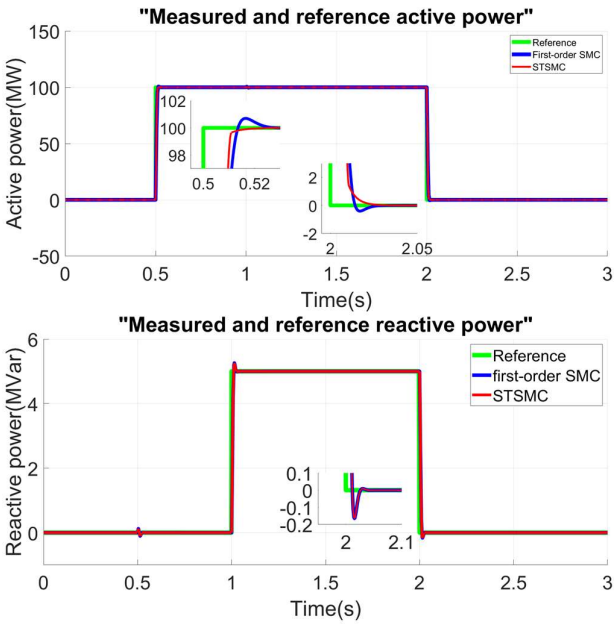

Fig. 8. Power responses for case A and B using first-order SMC and STSMC controllers: (a) active power (b) reactive power

Furthermore, the MMCs using STSMC can experience a better power balance in their legs and a lower level of CC consequently. It can be observed by a narrower power band in Fig. 9.

Fig. 10 shows the voltage profile in the system. the voltage drop is less than 1% in the worst case. In addition, error analysis in Fig. 11 shows that STSMC guarantees the return to the desired active-reactive power transfer setpoints.

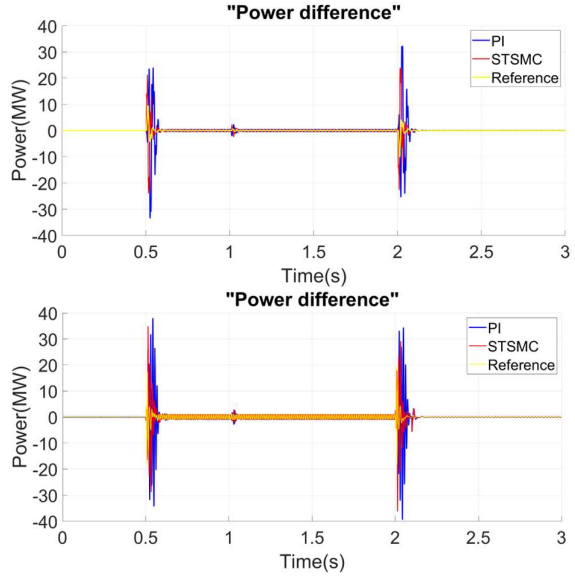

Fig. 9. Power difference using PI controller and STSMC: (a) in upper and lower leg in arm of each phase (b) between two legs

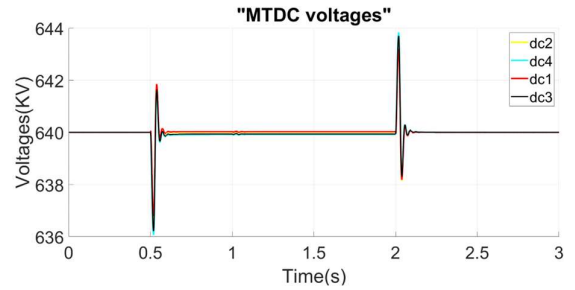

Fig. 10. Voltages in MTDC system

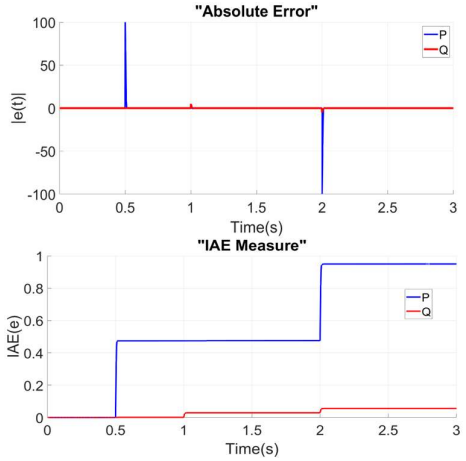

Fig. 11. Power transfer error evolution: (a) absolute error (b) integral of absolute error (IAE)

V. CONCLUSION

This paper deals with MTDC build-up with four MMCs, three of which are configured as slave and one as master. For all the converters, the first-order and the second-order SMC and conventional PI controllers are applied and compared. The controlling algorithm is analyzed with respect to AC power in different conditions such as power changes. Firstly, the mathematical model to represent the MMCs and the network is studied to analyze the interaction between AC and DC power systems. subsequently, the SMC for AC active and reactive power and energy balancing among legs and arms is designed to ensure the stable operation of the MTDC system. For a better evaluation of the control scheme, dq and αβ-frames are used instead of abc-frame. Results show that SMC can have a better response in terms of overshot, response time, power balance, circulating current, and stability if compared with traditional PI regulators. The stability analysis may be a topic of further studies.

VI. REFERENCES

[1] Freytes, Julian., "Small- signal Stability Analysis of Modular Multilevel Converters And Application to MMC –based Multi-Terminal DC Grids," *PhD thesis,* no. NTNU, 2017.

[2] Bahrman, Michael P., and Brian K. Johnson., "The ABCs of HVDC Transmission Technologies," *IEEE Power Energy Mag,* vol. 5, pp. 32-44, 2007.

[3] Johnson, M. Bahrman. B, "Topologies for VSC transmission," *Power and Energy Magazine,* vol. 5, no. IEEE, pp. 298-304, 2007.

[4] Oates, Colin, and Colin Davidson., "A Comparison of Two Methods of Estimating Losses In the Modular Multi-Level Converter," *European Conference on Power Electronics and Applications,* no. IEEE, pp. 1-10, 2011.

[5] A. Egea-Àlvarez, "Multiterminal HVDC Transmission Systems For Offshore Wind," *PhD thesis,* no. Universitat Politècnica de Catalunya (UPC), 2014.

[6] Egea-Alvarez, Agustí, Adriá Junyent-Ferré, and Oriol Gomis-Bellmunt., "Active and Reactive Power Control of Grid Connected Distributed Generation Systems," *Modeling and Control of Sustainable Power Systems,* no. Springer, pp. 47-81, 2012.

[7] Prieto-Araujo, Eduardo, et al., "Control design of Modular Multilevel Converters in normal and AC fault conditions for HVDC grids," in *Electric power system*, 2017.

[8] Qin, Jiangchao, and Maryam Saeedifard. , "Predictive Control of a Modular Multilevel Converter for a Back-to-Back HVDC System," *IEEE Trans,* p. 1538–1547, 2012.

[9] Sharifabadi, Kamran, et al., Application of modular multilevel converter on HVDC transmission systems, John Wiley & Sons, 2016.

[10] Slotine, Jean-Jacques E., and Weiping Li., "Sliding Control," in *Applied Non-linear Control*, Englewood Cliffs, 1991, pp. 276-310.

[11] Uddin, Waqar, et al., "Control of Output and Circulating Current of Modular Multilevel Converter Using a Sliding Mode Approach," *MDPI,* 2019.

[12] Khan, Mohammad Khalid., "Design and Application of Second Order Sliding Mode Control Algorithms," in *PhD thesis*, 2003.

[13] Sánchez-Sánchez, Enric, et al., "Analysis of MMC Energy-based Control Structures for VSC-HVDC Links," *JOURNAL OF EMERGING,* no. IEEE, 2018.

[14] H. Temesgen, "Control, Dynamics and Operation of Multi-terminal VSC-HVDC," *PhD thesis,* no. Norwegian University of Science and Technology (NTNU), 2012.

[15] Morched, Atef, Bjorn Gustavsen, and Manoocher Tartibi., "A Universal Model for Accurate Calculation of Electromagnetic Transients on Overhead Lines," *Trans. Power Del,* vol. 14, no. IEEE, pp. 1032- 1038, 1999.

[16] Ugalde-Loo, Carlos Ernesto, et al., "Open Access Simulation Toolbox for the Grid Connection of Offshore Wind Farms Using Multi-terminal HVDC," pp. 1-6, 2017.

[17] Debnath, Suman, et al., "Operation, Control, and Applications of the Modular Multilevel Converter: A review," *IEEE Trans. Power Electron,* vol. PP, pp. 1-1, 2014.

[18] Saad, Hani, et al., "On Resonances and Harmonics in HVDC-MMC Station Connected to AC grid," *IEEE Transactions on Power Delivery,* vol. 32, p. 1565–1573, 2017.